Original Article

JCBFM

Journal of Cerebral Blood Flow & Metabolism
2018, Vol. 38(6) 1060–1069

DOI: 10.1177/0271678X17713587
journals.sagepub.com/home/jcbfm
SAGE

Blockade and knock-out of CALHM1 channels attenuate ischemic brain damage

Abraham Cisneros-Mejorado[1,2], Miroslav Gottlieb[1,3], Asier Ruiz[1,2], Juan C Chara[1,2], Alberto Pérez-Samartín[1,2], Philippe Marambaud[4] and Carlos Matute[1,2]

Abstract

Overactivation of purinergic receptors during cerebral ischemia results in a massive release of neurotransmitters, including adenosine triphosphate (ATP), to the extracellular space which leads to cell death. Some hypothetical pathways of ATP release are large ion channels, such as calcium homeostasis modulator 1 (CALHM1), a membrane ion channel that can permeate ATP. Since this transmitter contributes to postischemic brain damage, we hypothesized that CALHM1 activation may be a relevant target to attenuate stroke injury. Here, we analyzed the contribution of CALHM1 to postanoxic depolarization after ischemia in cultured neurons and in cortical slices. We observed that the onset of postanoxic currents in neurons in those preparations was delayed after its blockade with ruthenium red or silencing of *Calhm1 gene* by short hairpin RNA, as well as in slices from CALHM1 knockout mice. Subsequently, we used transient middle cerebral artery occlusion and found that ruthenium red, a blocker of CALHM1, or the lack of CALHM1, substantially attenuated the motor symptoms and reduced significantly the infarct volume. These results show that CALHM1 channels mediate postanoxic depolarization in neurons and brain damage after ischemia. Therefore, targeting CALHM1 may have a high therapeutic potential for treating brain damage after ischemia.

Keywords

Acute stroke, adenosine triphosphate, calcium, cell death mechanisms, excitotoxicity

Received 12 November 2016; Revised 14 April 2017; Accepted 11 May 2017

Introduction

Cerebral ischemia triggers a sequence of short and long molecular pathways that start with a cellular energy failure phenomena. The rapid decrease of oxygen (O_2) and glucose in the infarct region of ischemic tissue can trigger cellular death within a few minutes as a result of deregulation in ionic concentrations.[1] Specifically, ischemia causes postanoxic depolarization of cells, which subsequently leads to excessive release of neurotransmitters, such as glutamate and adenosine triphosphate (ATP).[2–6] Excessive release of ATP can cause neuronal and glial cell death via P2X7 receptor activation,[7–9] however, the mechanisms by which deleterious ATP is released during ischemia are only partially known. Some data support the involvement of pannexin hemichannels.[9,10] An unexplored contributor to unregulated pathways in brain ischemia is the calcium homeostasis modulator 1 (CALHM1). CALHM1 was recently identified as a physiologically important plasma membrane Ca^{2+}-permeable ion channel regulated by voltage and extracellular Ca^{2+} levels.[11] This channel regulates cortical neuronal excitability in response to reduced extracellular Ca^{2+} concentrations and it is also able to form a large pore in mouse cortical

[1]Achucarro Basque Center for Neuroscience, Departamento de Neurociencias and CIBERNED, Universidad del País Vasco (UPV/EHU), Leioa, Spain
[2]Neurotek-UPV/EHU, Parque Tecnológico de Bizkaia, Zamudio, Spain
[3]Institute of Neurobiology, Slovak Academy of Sciences, Kosice, Slovak Republic
[4]The Feinstein Institute for Medical Research, Manhasset, NY, USA

Corresponding author:
Carlos Matute, Departamento de Neurociencias, Universidad del País Vasco, 48940-Leioa, Spain.
Email: carlos.matute@ehu.es

neurons[11] as well as in the cells of the taste buds.[12] CALHM1, originally identified as a possible modifier of the age of onset of Alzheimer's disease,[13,14] is present in cerebral-cortical neurons whereby can also release ATP.[12] In this study, we have investigated the contribution of CALHM1 to postanoxic depolarization and cell death during cerebral ischemia. We found that the pharmacological inhibition or knockdown of Calhm1 provides protection in ischemia. The protective effects of blockers or silencing were corroborated using knockout (KO) animals for CALHM1, remarking their therapeutic potential for cerebral ischemia.

Materials and methods

Study approval and animals

Protocols for primary cultures, cortical slices, and middle cerebral artery occlusion (MCAO) using mice wild-type (WT) and CALHM1 KO mice, were approved by the Comité de Ética y Bienestar Animal (Animals Ethics and Welfare Committee) of the University of the Basque Country. All experiments were performed by trained personnel with legal permits, and conducted in accordance with the ARRIVE guidelines and the Directives of the European Union Council (Directive 2010/63/EU) and Spanish regulations (Real Decreto 53/2013) on animal ethics and welfare. WT mice were purchased to Harlan (Barcelona, Spain). CALHM1 knockout mice were developed in P.M.'s laboratory as previously detailed.[11,12] Calhm1 KO homozygous and WT littermates were maintained as separate lines (Calhm1−/− and +/+). Mice were provided by Dr Marambaud and genotyping was performed in his laboratory and confirmed by RT-qPCR (Real-time quantitative polymerase chain reaction) following procedures already published elsewhere.[15,16]

All possible efforts were made to minimize animal suffering and the number of animals used.

Cortical neuronal culture preparations and transfection with short hairpin RNA

Primary cultures of neurons were established according to previously described procedures.[17,18] Briefly, neurons derived from cortical lobes of C57BL/6 mice embryos (18 days of gestational age) were resuspended in B27 neurobasal medium plus 10% Fetal Bovine Serum (FBS) and seeded onto poly-L-ornithine-coated 24-well plates bearing 12-mm-diameter coverslips at 2×10^5 cells per well. The medium was replaced by serum-free, B27-plus antibiotic-antimycotic and glutamine (2 mM)-supplemented neurobasal medium 24 h later and cultures were maintained at 37°C and 5% CO_2.

For knockdown of *Calhm1* gene by short hairpin RNA (shRNA), 4×10^6 neurons were transfected in suspension before plating with 3 μg of pGFP-C-shLenti vector (Origene Technologies, Rockville, MD) using Rat Neuron Nucleofector Kit (Lonza, Basel, Switzerland) according to the manufacturer instructions, and plated and maintained as described above. Control (scrambled shRNA) and silenced neurons were used at 7–21 days in vitro. Neurons carrying out the transgene were identified using a high-resolution digital B/W CCD camera (ORCA; Hamamatsu Photonics Iberica, Barcelona, Spain) equipped with epifluorescence. We used at least four neuronal cultures for each experimental condition ($5–10 \times 10^4$ cells/well). Quantification of transfected and nontrasfected cells resulted in an efficiency of transfection typically around 40% (38.7% ± 9.4% and 37.5% ± 4.9% for neurons with targeted and scrambled shRNA, respectively).

Oxygen and glucose deprivation in neuronal cultures

Oxygen and glucose deprivation (OGD) (2 h) was achieved using a Modular Incubator Chamber (MIC-101) (Billups-Rothenberg), by replacing O_2 with N_2 and external glucose (10 mM) with sucrose, and adding iodoacetate (IAA; 100 μM) to block glycolysis plus the oxidative phosphorylation inhibitor antimycin (0.25 μmol/L) in an extracellular solution containing (in mM) NaCl (140), KCl (5), $CaCl_2$ (2.5), $MgCl_2$ (1), and HEPES (10). Cell survival was determined 24 h after restoring normoxia and glucose, with calcein-AM (Promega, Madison, WI) as previously described[8] using a Synergy-HT fluorimeter (BioTek Instruments, VT). Conversely, cell death was assessed by measuring the release of Lactate Dehydrogenase (LDH), using the Citotox 96 colorimetric assay (Promega). Absorbance was read at 490 nm, and LDH release was expressed as the proportion of release caused by OGD. All experiments with LDH and calcein were performed in at least four independent assays and with at least six wells for each condition.

Brain cortical slices

Cortical slices were obtained from 12 - to 20-weeks old C57BL/6 or CALHM1-KO male. Briefly, mice were anesthetized with isoflurane, then, brains dissected out and coronal sections of 300 μm prepared on a vibratome (Pelco 100, Pelco, Clovis, CA) in ice-cold artificial cerebrospinal fluid containing (in mmol/L) NaCl (126), $NaHCO_3$ (24), NaH_2PO_4 (1), KCl (2.5), $CaCl_2$ (2.5), $MgCl_2$ (2), and D-glucose (10; bubbled with 95% O_2/5% CO_2) at pH 7.4. After collection, slices were transferred into an artificial cerebrospinal fluid solution at 37°C for at least 30 min, and then used for

electrophysiology recordings. Ischemia in cortical slices was mimicked by replacing glucose in the artificial cerebrospinal fluid with 10 mM sucrose and bubbling continuously with 95% N_2/5% CO_2. The artificial cerebrospinal fluid and ischemia solutions were maintained at 37°C during the recordings.

Electrophysiology

Whole-cell patch clamp recordings of ionic currents of cultured neurons or cortical slices were performed with a Multiclamp 700B amplifier (Molecular Devices, Sunnyvale, CA). Neurons were constantly perfused with external solution containing (in mmol/L) NaCl (140), KCl (5), $CaCl_2$ (2.5), $MgCl_2$ (1), HEPES (10), and glucose (10) at pH 7.3 (NaOH). The pipette solution contains (in mmol/L) potassium gluconate (140), $CaCl_2$ (1), $MgCl_2$ (2), HEPES (10), EGTA (10), Na-GTP (0.2), and Mg-ATP (2) at pH 7.3 (KOH). Electrophysiological recordings in slices were made in layer V pyramidal neurons of motor cortex region, using electrodes of 2–4 MΩ resistance. The slices were under continuous perfusion (1.5 mL/min) with an external solution (bubbled with 95% O_2/5% CO_2) containing (in mmol/L) NaCl (126), KCl (2.5), $CaCl_2$ (2.5), $MgCl_2$ (2), and D-glucose (10) at pH 7.4. Data were digitized at 5 kHz and lowpass filtered at 0.2 kHz.

Transient MCAO

Transient focal ischemia was induced by a 60 min intraluminal occlusion of the middle cerebral artery (MCAO) followed by reperfusion in adult (3–6 month-old, 25–32 g body weight) male WT or CALHM1 KO mice as reported previously.[11,19] After applying exclusion criteria (see below) six animals were finally used for quantification in each experimental group. Briefly, the animals were anesthetized with 4% (v/v) isoflurane and maintained under 1.2% (v/v) isoflurane with a facemask. MCAO was performed by inserting a 6-0 nylon monofilament via the right external carotid artery into the internal carotid artery to block the origin of the MCAO. The MCAO was confirmed by measuring local cerebral blood flow using a laser-Doppler flowmeter (PeriFlux System 5000, Perimed AB, Järfälla, Sweden), and only mice with blood flow reduced by >85% were used for experiments (five animals were excluded with this criteria: 1 WT and 2 KO mice, and 2 mice treated with RuR). Animals were sutured and placed in their cages with ad libitum access to food and water. After 50 min of occlusion, the animals were reanesthetized, and then at 60 min the filament was removed to allow reperfusion for 3 days. The Bederson et al.[20] scale was used, by an independent researcher without role during MCAO surgery, to determine the neurological symptoms caused by the MCAO: 0 for undetectable neurologic deficits; 1 for forelimb flexion and torso rotated towards the contralateral side when the animal is lifted by the tail; 2 for the same deficit grade 1 plus a decreased resistance to lateral push; 3 for the same deficit grade 2 plus unilateral move; and 4 no spontaneous walking and a depressed level of consciousness. Animals with initial neurologic deficits lower than score 2 were excluded from the study (four animals were excluded with these criteria: 1 WT and 1 KO mice, and 2 mice treated with RuR). Neurological score was measured at 60 min, then at 24, 48, and 72 h after MCAO. In addition, animals showing signs of subarachnoid hemorrhage/blood vessel rupture, heart failure during surgery, and severe weight-loss, or that died during recirculation treatment were excluded from analysis, and exclusion of any data was done prior to unblinding (seven animals were excluded with these criteria: 3 WT and 2 KO mice, and 2 mice treated withRuR).

Analysis of cerebral infarct size

Mice were anesthetized with chloral hydrate anesthesia followed by decapitation, at 72 h after MCAO. Then, the brains were removed, and the forebrain was sliced into 2-mm-thick coronal sections (Brain Matrices, Ted Pella, Inc., CA). To determine brain infarct size, sections were stained with 1% (w/v) 2,3,5-triphenyltetrazolium chloride (TTC; Sigma–Aldrich, Madrid, Spain) saline solution at 37°C for 10–15 min. The infarct volume of the brain slice was measured using Image J software (National Institutes of Health, Bethesda, MD). The average infarct area (mm^2) in each section was calculated by the following formula: (infarct area on the anterior surface + infarct area on the posterior surface) / 2. Infarct volumes (mm^3) were calculated by the sum of all the section areas and multiplying by the slice thickness. The corrected infarct volume to compensate brain edema was calculated by applying the formula: (nonischemic volume/ischemic volume) × infarct volume.[21] Moreover, coronal cryosections after TTC staining and fixing were cryostat cut at 10 µm, sections mounted onto gelatinized microscope slides, and stored at −20°C until next staining with Fluoro-Jade C (FJ; Merck Millipore, Madrid, Spain) a marker for degenerating neurons.[22] Sections were air dried and stained with 0.0001% FJ for 20 min, washed, dried, and coverslipped with DPX. Series of microphotographs were taken from four regions of the ipsilateral side, two parts of the cerebral cortex and two areas from the striatum, with a 20× objective using Zeiss Axoplan microscope (Madrid, Spain), and FJ-positive cells were counted by Image J software (Image Pro Plus 7, Media Cybernetics, Rockville, MD).

Drug treatment

For in vivo experiments, saline solution (vehicle) or ruthenium red were prepared in aliquots and then coded with an alphanumeric name by an independent researcher. The aliquots have the final volume to inject (200 μL; i.p.) and were administered starting at 30 min after the onset of ischemia and thereafter, every 12 h during 3 days. WT mice (C57BL/6) were randomly assigned to each treatment and blinded analysis was of outcomes completed by the participating researcher.

Data analysis

All data are reported as mean ± SEM. For electrophysiology with cortical slices and in vivo experiments, we calculated the sample size (n) of animals needed in each experimental group taking into consideration the variability of measurements of each experimental paradigm and the incidences that influence the procedures like mortality during/or postsurgery or culling by symptoms of pain in mice in accordance with the ethics protocols of Animals Ethics and Welfare Committee. Animals were randomized to treatment according to local practice in participating centers, and following an experimental design of randomized blocks.[23] We used Origin (v.8.5) (Microcal Software; Madrid, Spain), a standard software for power calculation in the study of comparison between groups, to conduct a sample size design. In accordance with previous studies with similar experimental procedures,[8,10,24] we assumed an effect size of around 1.9 (Cohen's d estimation calculus), and a minimum of six animals required to provide a power of 80% in detecting changes between means of groups in the in vivo experiments with significance level of 0.05. For the MCAO experiments, we also estimated the number of animals required taking into account the major incidences in this procedure, using the empirical formula $x = \eta[(1 - a/100)(1 - b/100)\ (c/100)]^{-1}$,[25] where x is the final number of animals used, η is the minimum number of animals that allows distinguishing differences between means, as calculated above, and a, b, and c representing mortality (30%), hemorrhage (20%), and small infarcts (10%), respectively according to similar surgery procedures.[26,27] One-way analysis of variance test with Fisher's post hoc and t-test were performed to compare between groups. The Kolmogorov–Smirnov method was used to prove the normality of data. For nonparametric data we used the Friedman test. Data were analyzed using GraphPad Prism v. 4 (or Instat 3) software (GraphPad software; San Diego, CA) or Origin 8.5 (Microcal Software).

Results

Blockade of CALHM1 decreases ionic currents in cultured neurons

We initially evaluated the contribution of CALHM1 channels in the current–voltage relationship in isolated neurons. Thus, induction of ionic currents were under a protocol of voltage pulses (Figure 1(a)) which permits evaluating Na^+-currents, K^+-currents, and the currents in the steady state. Application of CALHM1 antagonists ruthenium red (RuR, 20 μM) and Zn^{2+} (20 μM) decreased uniquely the currents in the steady state (Figure 1(d)) but not in Na^+ or K^+ currents (Figure 1(b) and (c)), in accordance with previous studies.[12] We found a significant reduction of almost 40% in the currents in the steady state for both, RuR and Zn^{2+}, suggesting that CALHM1 channel is activated at positive potentials, and contribute to the macroscopic ion currents without altering the typical Na^+/K^+ currents in isolated neuronal cultures preparations.

Ischemia activates CALHM1 channels in cultured neurons

To evaluate the contribution of CALHM1 channels in ischemic conditions, we measured the ionic current triggered by in vitro ischemia as reported in previous studies.[8,11] In cultured neurons, ischemia induced an inward current that became evident 2.27 ± 0.31 min later (Figure 2(a)). Application of the CALHM1 blocker, RuR (20 μM) at the onset of ischemia greatly increased the latency up to 3.99 ± 0.29 min (Figure 2(a)). Accordingly, knockdown of CALHM1 with shRNAs, robustly delayed the start rise of the postanoxic currents (sh-CALHM1, 4.31 ± 0.29 min; Figure 1(a)). The use of scramble shRNAs (nontarget, NT) did not significantly change the onset of ionic currents (Figure 1(a)). Notably, CALHM1 blocker (RuR, 20 μM) was effective in reversing the ischemic ionic current when applied immediately after its onset (Figure 2(b)), suggesting that CALHM1 are activated during early ischemia and contribute to the depolarization caused in neurons.

Knockdown of CALHM1 reduces cell death induced by OGD in cortical neurons

In order to study the involvement of CALHM1 channels in cell death induced by OGD, neurons transfected with CALHM1-silencing shRNAs were subjected to OGD for 120 min. Toxicity and cell survival was determined 24 h later by measuring LDH release and calcein fluorescence, respectively. We found that silencing of CALHM1 decreases the LDH release by 13% (Figure 3(a)) while cell viability increased

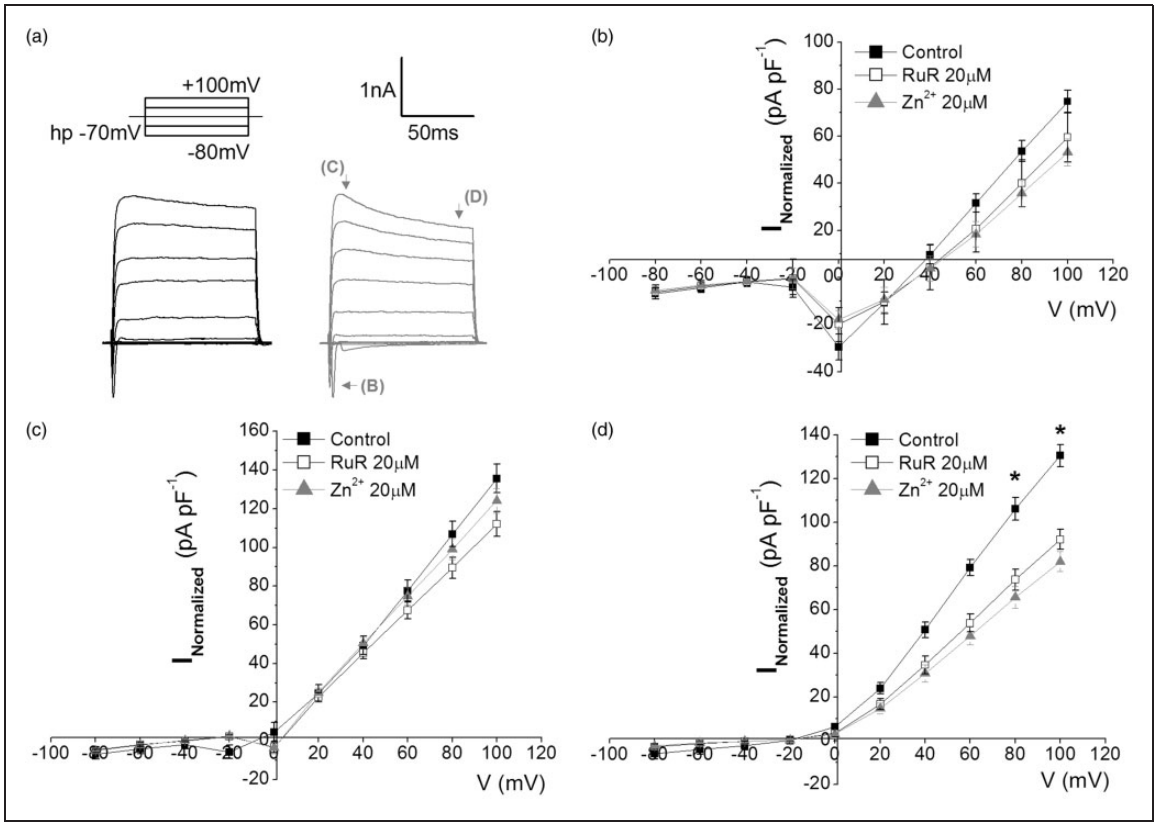

Figure 1. Blockade of CALHM1 reduces ionic currents, at positive potentials. (a) Representative traces of currents induced by a voltage pulse protocol (above) ranging from −80 to + 100 mV in the absence (black) and presence (gray) of CALHM1 blocker, Ruthenium Red 20 μM (RuR). (b–d) shows the relationship of the current density versus voltage (IV) to neurons in the absence (control) and in presence of two blockers of CALHM1 channel, RuR and Zn^{2+}. In (b–d), the IV curves shows Na^{+}-currents (corresponding to inward current depicted with arrow *i* in a), K^{+}-currents (corresponding to outward current depicted with arrow *ii* in a) and currents in steady state (corresponding to outward current depicted with arrow *iii* in a). The graphs show the average ± SEM. $^{*}P < 0.05$ ($n = 6$ for each case). One-way analysis of variance test with Fisher's post hoc test were performed.

about 19%, as compared with neurons expressing NT shRNAs. These results indicate that activation of CALHM1 channels during ischemia contribute to neuronal demise.

Blockade or gene deletion of CALHM1 channels reduces the ionic current induced by ischemia in neurons in cortical slices

We next examined the contribution of CALHM1 to ischemic ionic current in cortical neurons in brain slices (250 μm), a more integral preparation than neuronal cultures. As in the latter, inducing ischemia in brain slices activated a large inward current with a latency of 5.2 ± 0.7 min (Figure 4). However, in the presence of CALHM1 antagonist RuR (20 μM) the latency increased to 7.7 ± 0.9 min. Importantly, we observed a similar delay in the onset of the postanoxic currents in slices from CALHM1 KO mice (8.2 ± 1.4 min; Figure 4). These results indicate that CALHM1 channels contribute to the onset of the postanoxic depolarization leading to neuronal demise in brain slices preparations, which is delayed by blockage or gene deletion of CALHM1.

Blockade and genetic ablation of CALHM1 channels are protective after MCAO

To evaluate the relevance to stroke of the observations described above, we explored the effect of the CALHM1 antagonist RuR as well as of ablating CALHM1 in KO mice on postischemic injury after transient MCAO. Analysis of cerebral ischemic damage with TTC staining shows that damage was reduced in both instances (Figure 5). In WT animals (control) the volume of damage was 51.39 ± 5.7 mm^3 after 3 days of MCAO, while in CALHM1 KO the volume was reduced to 36.64 ± 6.1 mm^3 (KO, Figure 5). Interestingly, the application of RuR (1 mg/kg) resulted in higher protection (volume of damaged tissue 20.06 ± 2.8 mm^3).

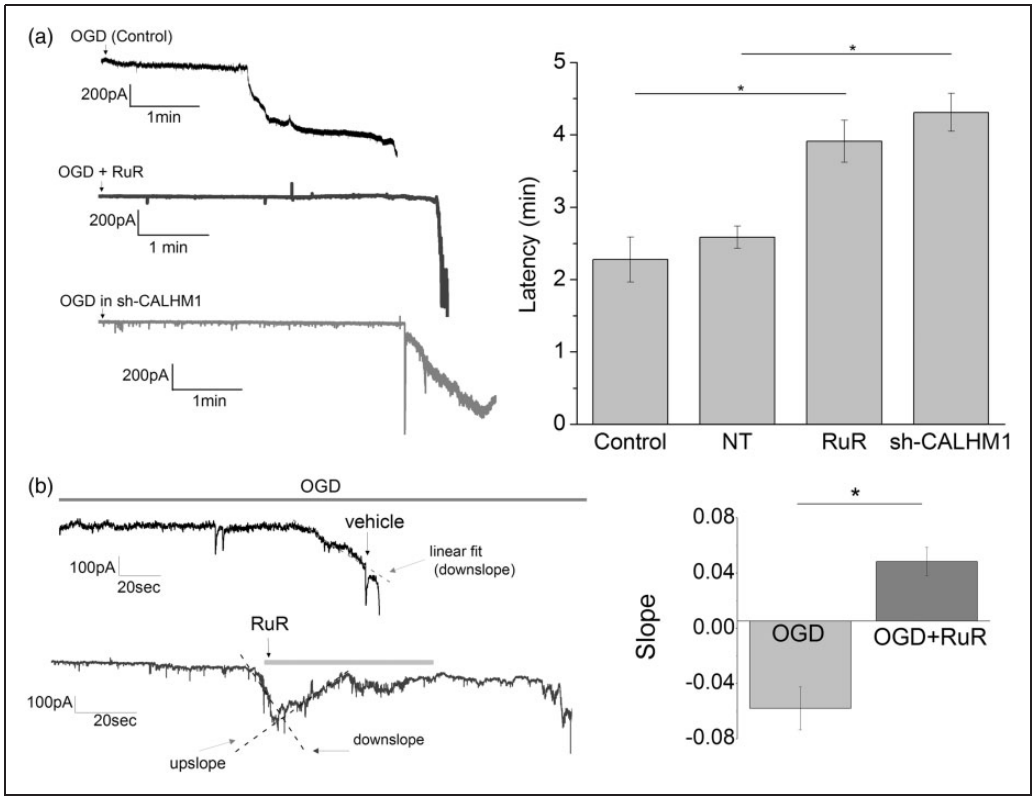

Figure 2. Pharmacological blockade or silencing of CALHM1 channels delays postanoxic ionic currents in cultured neurons. (a) At left, representative recordings obtained in whole-cell configuration at −70 mV of ionic currents induced by ischemia (OGD) in cultured neurons with no treatment (control; $n = 14$), and after pharmacological blockade of CALHM1 with RuR (20 μM; $n = 8$) or silencing of CALHM1 with shRNA (sh-CALHM1; $n = 7$). At right, histogram showing the latency of onset of ischemic ionic current in each of the aforementioned conditions. NT column represents values after transfection of plasmid with irrelevant shRNA ($n = 6$). (b) At left, representative traces of currents induced by OGD in cultured neurons in the absence (vehicle) or presence of CALHM1 inhibitor RuR (20 μM). Note the recovery when RuR is added in the first stages of postanoxic ion currents. At right, the value of slope (downslope and upslope) fitted to ischemic ionic current in the absence (OGD, vehicle, $n = 9$) or presence of CALHM1 inhibitor, RuR ($n = 8$). Data show the mean ± SEM. $^*P < 0.05$. One-way analysis of variance test with Fisher's post hoc and *t*-test test were performed.

In addition, the neurological score at 1 h after MCAO was similar in all tested animals, control, KO mice, and mice treated with RuR. At later postischemic time points, the score improved progressively until 3 days of reperfusion. In particular, treatment with RuR ameliorated symptoms significantly as compared to vehicle-treated mice.

Subsequently, we quantified the number of degenerated neurons, as stained with FJ, in cryostat sections at the level of the center of the infarct area (typically with slice 3 from the top of the panel illustrating TTC staining in Figure 5(a)). This analysis revealed that there were 694.5 ± 103 cells/mm^2 of FJ-positive cells in WT mice (Figure 6) at 3 days after ischemia, while CALHM1 KO animals subjected to ischemia displayed a lower number of positive-stained cells (445.4 ± 73 cells/mm^2) as did RuR-treated animals (363.1 ± 52 cells/mm^2, Figure 6).

Discussion

In this study, we showed that cortical neurons in dissociated cultures and in brain slices have functional CALHM1 channels that are readily activated after ischemia and contribute to postanoxic depolarization. In addition, we provide evidence that blockade of CALHM1 channels, knockdown of its encoding gene with shRNA or its deletion attenuates postischemic neuronal death and tissue damage in vitro. Finally, we found a robust decrease in infarct volume and cell death in CALHM1 KO mice and following treatment with RuR after the onset of ischemia subsequent to transient MCAO. Together, these results show that the activation of CALHM1 channels substantially contributes to anoxic depolarization and cell death after brain ischemia.

Loss of membrane potential occurs during brain ischemia, which leads to anoxic depolarization[4,28,29]

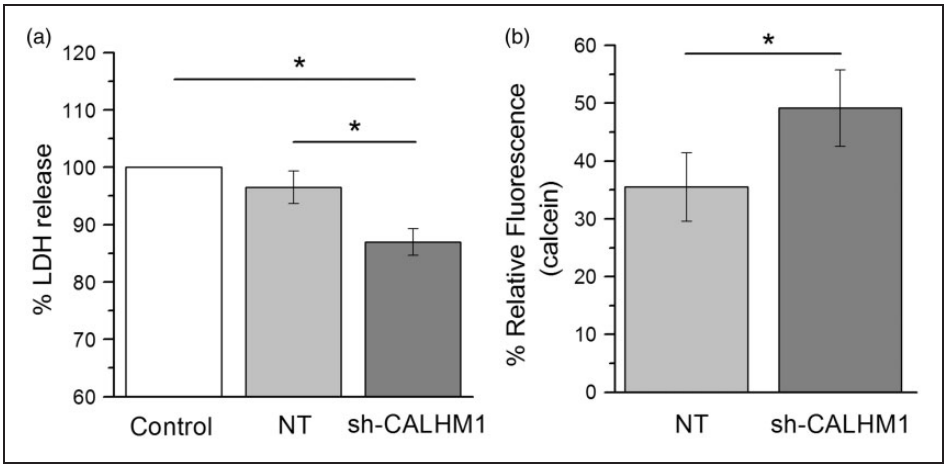

Figure 3. Silencing of CALHM1 promotes cell survival against OGD in cortical neurons. (a) Percentage of LDH release OGD-induced in cultures subjected to 120 min of OGD and 24 h of reoxygenation. The histogram shows the percentage normalized at control group (neurons without treatment exposed to OGD), cultures transfected with noneffective shRNA cassette (NT; control of transfection) and cultures transfected with short hairpin RNA specific for CALHM1 (sh-CALHM1). Data points originate from four independent experiments with 12 replicates per condition in each individual assay. (b) Relative fluorescence measured with Calcein-AM (1 μM) to quantify cell viability at 24 h after OGD (120 min) in NT and sh-CALHM1 groups. The histogram show the mean normalized at OGD group (level zero of fluorescence). Four independent experiments were carried out with six replicates per condition in each individual assay. All data are expressed as the mean ± SEM. *$P < 0.05$, one-way analysis of variance test with Fisher's post hoc or *t*-tests were performed for each case.

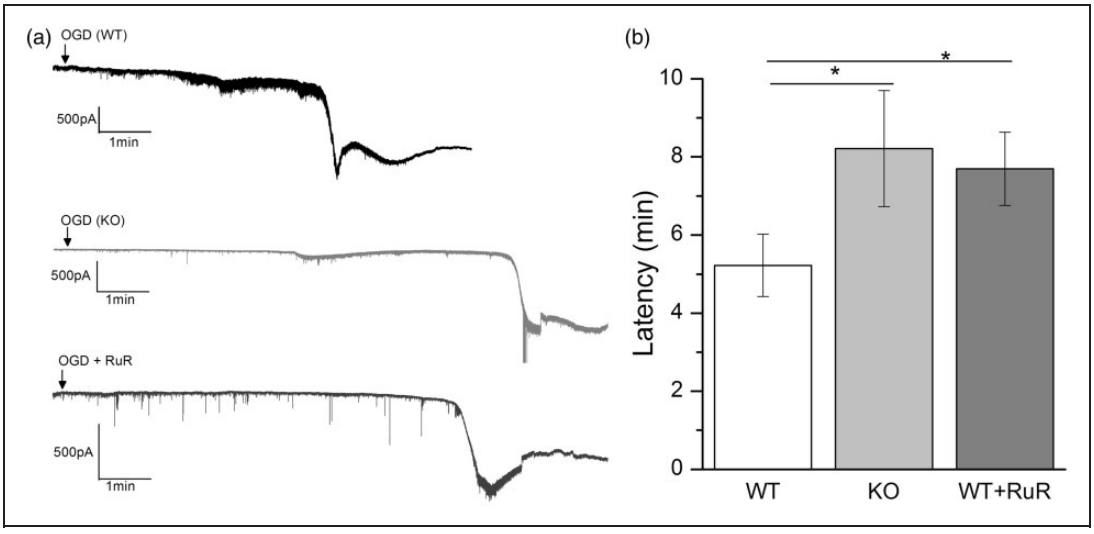

Figure 4. Blockade or lack of CALHM1 channels delays ischemic ionic currents in cortical slices. (a) Representative electrophysiological recording in whole-cell configuration (holding potential at −70 mV), of ischemic (OGD) ionic current in cortical neurons in brain slices (250 μm) in wild-type (WT) mice, CALHM1 KO (KO) mice or in WT in presence of CALHM1 blocker RuR (20 μM), respectively. (b) Histogram of the latency of the onset of ischemic ionic current in WT ($n = 13$), KO ($n = 12$) and in WT in presence of RuR ($n = 10$). Data show the mean ± SEM. *$P < 0.05$ versus control (WT). One-way analysis of variance test with Fisher's post hoc test were performed.

that promotes massive release of ATP (reviewed in literature[30,31]). In the case of ATP, its excess during ischemia results in excitotoxic death of neurons and oligodendrocytes via activation of P2X7 receptors.[8–10] However, the mechanisms of ATP release during ischemia are not well known yet. P2X7 receptor, a member of the family of ATP-gated channels,[32,33] is involved in nonvesicular release of ATP since this receptor can form a large pore upon activation, allowing the passage of organic cations and molecules of up

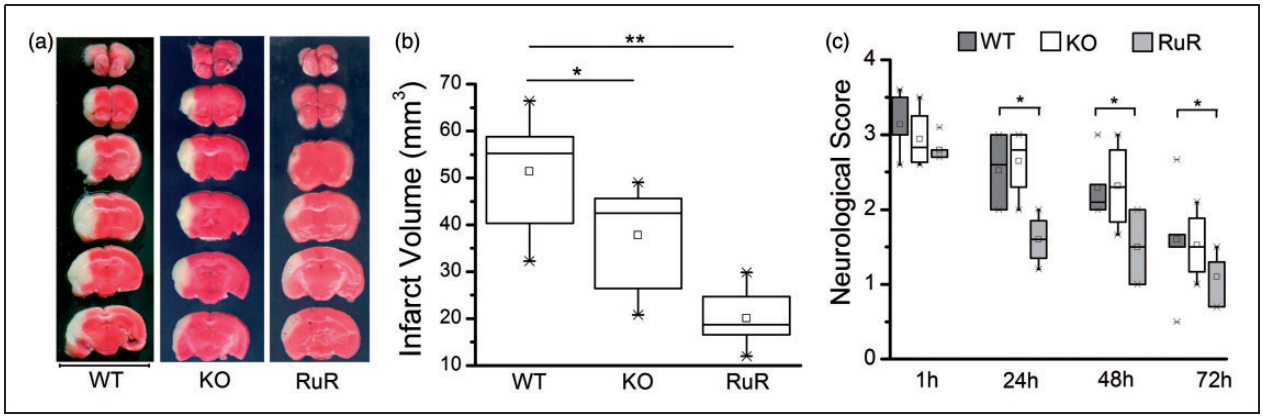

Figure 5. Genetic ablation of CALHM1 or treatment with ruthenium red (RuR) reduces brain damage after transient middle cerebral artery occlusion (MCAO). (a) Representative 2,3,5-triphenyltetrazolium chloride (TTC)–stained sections depicting damage in brains from wild-type mice (WT), knockout CALHM1 mice (KO), and mice treated with ruthenium red (RuR, 1 mg/kg, i.p.). RuR or vehicle was administered beginning at 30 min after the onset of ischemia and later every 12 h during 3 days of reperfusion, until sacrifice. Bar = 10 mm. (b) Infarct volume calculated from TTC-stained slices in WT, KO and RuR-treated mice ($n = 6$ for each experimental group). (c) Neurological score at 1, 24, 48, and 72 h reperfusion ($n = 6$ for each data point). *$P < 0.05$, **$P < 0.001$. The box chart graphs (b and c) show the distribution of data with mean (square symbol into box), median (horizontal line dividing the box), and the interquartile range (cross mark). One-way analysis of variance test with Fisher's post hoc and the nonparametrical Friedman tests were used.

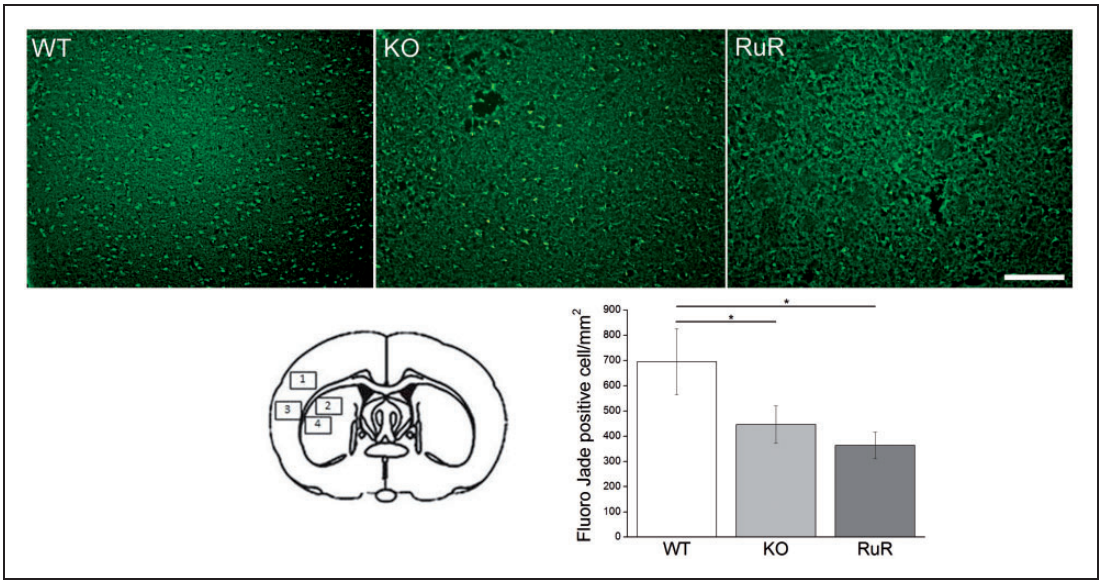

Figure 6. CALHM1 blockade or deletion diminishes the number of dying neurons after MCAO. Above, the representative micrographs of infarct core in the cerebral cortex stained with Fluoro-Jade C in wild type (WT), KO-CALHM1 (KO) and in wild type with RuR (RuR). Images were taken from region 3 on the drawing illustrated, below at left. Note a reduction of FJ-positive neurons in knockout mice and RuR-treated mice. The histogram illustrates the mean ± SEM of dying neurons in all four regions indicated in the drawing at the left. Scale bar: 100 μm. *$P < 0.05$ ($n = 6$ animals per condition and 4 slices for WT, 3 slices for KO, and 3 slices for RuR animal). One-way analysis of variance test with Fisher's post hoc test were used.

to 900 Da, and the leakage of metabolites including ATP.[34,35] A role in ATP release has also been assigned to pannexin 1 channels (Panx1), heavily expressed in the CNS, which are large pore ion channels that mediate ATP release.[36,37] On the other hand, CALHM1 is also involved in ATP release. Originally identified as a possible modifier of the age of onset of Alzheimer's disease,[13,14] CALHM1 is also able to form a large pore in mouse cortical neurons[11] as well as in the cells of the taste buds and in cerebral-cortical neurons.[12]

We hypothesized that the rise in ATP concentration or the pathways triggered during ischemia might be modulated by the activation of CALHM1, which in turn can induce anoxic cell depolarization. Indeed, we found that inhibition of CALHM1 partially blocked the ionic currents triggered by ischemic conditions and prevented cultured neurons from dying. Curiously, we observed a stronger protective effect with the CALHM1 blocker RuR as compared to gene silencing or deletion in KO mice. This is probably due to interaction of RuR with other channels and receptors mediating ischemic injury. Indeed, RuR also blocks transient receptor potential cation channels, which are known to be activated by ischemia and mediate tissue damage, as well as CalHM2-3.[38,39] In addition, RuR attenuates vascular dementia in an experimental model of diabetes in rats, an effect that appears to be mediated by blocking of ryanodine receptors.[40] Finally, early blockade of CALHM1 after the onset of ischemia may limit the subsequent propagation of spreading waves of depolarization in the peri-infarct area.[41] Neuroprotection was partial as other receptors and channels are involved in postanoxic depolarization and cell death (for recent reviews see literature[30,31]). This includes P2X7 receptors or Panx1.[8–10] In turn, the expression of CALHM1 correlates with that of P2X7 in a painful diabetic neuropathy model whereby the rise of ATP levels, and of P2X7 receptor expression in glia could be reverted in part by inhibiting CALHM1.[42] It is conceivable that a similar pathway can be active during brain ischemia, although this possibility needs to be assessed.

In summary, we show that the CALHM1 activation importantly contributes to postanoxic depolarization and cell damage in vitro and in vivo brain ischemia, and that its blockade, knockdown or deletion confers robust neuroprotection. Therefore, targeting the CALHM1 has a therapeutic potential to attenuate the consequences of stroke.

Funding

The author(s) disclosed receipt of the following financial support for the research, authorship, and/or publication of this article: This work was supported by MINECO (SAF2013-45084-R and SAF2016-75292-R), CIBERNED, Gobierno Vasco and Universidad del País Vasco. MG was partially supported by VEGA 2/0012/15, Slovak Republic.

Acknowledgments

The authors would like to thank to H. Gómez, S. Marcos, and E. Muñoz for technical assistance.

Declaration of conflicting interests

The author(s) declared no potential conflicts of interest with respect to the research, authorship, and/or publication of this article.

Authors' contributions

AC-M, MG, AP-S, and CM designed experiments. AC-M, MG, AR, and JCCh carried out the experiments. PM provided genotyped CALHM KO mice and advice. AC-M and CM wrote the initial manuscript. All authors supervised and contributed to the final manuscript. Materials related to this paper can be accessed.

References

1. Thompson RJ, Zhou N and MacVicar BA. Ischemia opens neuronal gap junction hemichannels. *Science* 2006; 312: 924–927.
2. Braun N, Zhu Y, Krieglstein J, et al. Upregulation of the enzyme chain hydrolyzing extracellular ATP after transient forebrain ischemia in the rat. *J Neurosci* 1998; 18: 4891–4900.
3. Jurányi Z, Sperlágh B and Vizi ES. Involvement of P2 purinoceptors and the nitric oxide pathway in purine outflow evoked by short-term hypoxia and hypoglycemia in rat hippocampal slices. *Brain Res* 1999; 823: 183–190.
4. Melani A, Turchi D, Vannucchi MG, et al. ATP extracellular concentrations are increased in the rat striatum during in vivo ischemia. *Neurochem Int* 2005; 47: 442–448.
5. Rossi DJ, Brady JD and Mohr C. Astrocyte metabolism and signaling during brain ischemia. *Nat Neurosci* 2007; 10: 1377–1386.
6. Yenari MA, Kauppinen TM and Swanson RA. Microglial activation in stroke: therapeutic targets. *Neurotherapeutics* 2010; 7: 378–391.
7. Matute C, Torre I, Pérez-Cerda F, et al. P2X7 receptor blockade prevents ATP excitotoxicity in oligodendrocytes and ameliorates experimental autoimmune encephalomyelitis. *J Neurosci* 2007; 27: 9525–9533.
8. Arbeloa J, Pérez-Samartín A, Gottlieb M, et al. P2X7receptor blockade prevents ATP excitotoxicity in neurons and reduces brain damage after ischemia. *Neurobiol Dis* 2012; 45: 954–961.
9. Domercq M, Perez-Samartin A, Aparicio D, et al. P2X7 receptors mediate ischemic damage to oligodendrocytes. *Glia* 2010; 58: 730–740.
10. Cisneros-Mejorado A, Gottlieb M, Cavaliere F, et al. Blockade of P2X7 receptors or pannexin-1 channels similarly attenuates postischemic damage. *J Cereb Blood Flow Metab* 2015; 35: 843–850.
11. Ma Z, Siebert AP, Cheung KH, et al. Calcium homeostasis modulator 1 (CALHM1) is the pore-forming subunit of an ion channel that mediates extracellular Ca2+ regulation of neuronal excitability. *PNAS* 2012; 109: E1963–E1971.
12. Taruno A, Vingtdeux V, Ohmoto M, et al. CALHM1 ion channel mediates purinergic neurotransmission of sweet, bitter and umami tastes. *Nature* 2013; 495: 223–226.
13. Dreses-Werringloer U, Lambert JC, Vingtdeux V, et al. A polymorphism in CALHM1 influences Ca2+ homeostasis, Aβ levels, and Alzheimer's disease risk. *Cell* 2008; 133: 1149–1161.
14. Lambert JC, Sleegers K, Gonzalez-Perez A, et al. The CALHM1 P86L polymorphism is a genetic modifier of

age at onset in Alzheimer's disease: a meta-analysis study. *J Alzheimers Dis* 2010; 22: 247–255.
15. Vingtdeux V, Chang EH, Frattini SA, et al. CALHM1 deficiency impairs cerebral neuron activity and memory flexibility in mice. *Sci Rep* 2016; 12: 24250.
16. Vingtdeux V, Chandakkar P, Zhao H, et al. CALHM1 ion channel elicits amyloid-β clearance by insulin-degrading enzyme in cell lines and in vivo in the mouse brain. *J Cell Sci* 2016; 128: 2330–2338.
17. Larm JA, Cheung NS and Beart PM. (S)-5-Fluorowillardiine-mediated neurotoxicity in cultured murine cortical neurones occurs via AMPA and kainate receptors. *Eur J Pharmacol* 1996; 314: 249–254.
18. Cheung NS, Pascoe CJ, Giardina SF, et al. Micromolar L-glutamate induces extensive apoptosis in an apoptotic-necrotic continuum of insult-dependent, excitotoxic injury in cultured cortical neurones. *Neuropharmacology* 1998; 37: 1419–1429.
19. Longa EZ, Weinstein PR, et al. Reversible middle cerebral artery occlusion without craniectomy in rats. *Stroke* 1989; 20: 84–91.
20. Bederson JB, Pitts LH, Tsuji M, et al. Rat middle cerebral artery occlusion: evaluation of the model and development of a neurologic examination. *Stroke* 1986; 17: 472–476.
21. Callaway J, Knight M, Watkins D, et al. A novel, rapid, computerised method for quantitation of neuronal damage in a rat model of stroke. *J Neurosci Methods* 2000; 102: 53–60.
22. Schmued LC, Stowers CC, et al. Fluoro-Jade C results in ultra high resolution and contrast labeling of degenerating neurons. *Brain Res* 2005; 1035: 24–31.
23. Mead R, Gilmour SG and Mead A. *Statistical principles for the design of experiments: Applications to real experiments*. Cambridge: Cambridge University Press, 2012, p.36.
24. Tu W, Xu X, Peng L, et al. (2010). DAPK1 interaction with NMDA receptor NR2B subunits mediates brain damage in stroke. *Cell* 2010; 140: 222–234.
25. Rojo A. Cálculo del tamaño muestral en procedimientos de experimentacioón con animales. Valoración de las incidencias. In: *Animales de Laboratorio*. Revista de la Sociedad espaola para las ciencias del animal de laboratorio, vol. 62, 2014, pp.31–33.
26. Lindner MD, Gribkoff VK, Donlan NA, et al. Long-lasting functional disabilities in middle-aged rats with small cerebral infarcts. *J Neurosci* 2003; 23: 10913–10922.
27. Spratt NJ, Fernandez J, Chen M, et al. Modification of the method of thread manufacture improves stroke induction rate and reduces mortality after thread-occlusion of the middle cerebral artery in young or aged rats. *J Neurosci Methods* 2006; 155: 285–290.
28. Jurányi Z, Sperlágh B and Vizi ES. Involvement of P2 purinoceptors and the nitric oxide pathway in purine outflow evoked by short-term hypoxia and hypoglycemia in rat hippocampal slices. *Brain Res* 1999; 823: 183–190.
29. Frenguelli BG, Bruno G, et al. Temporal and mechanistic dissociation of ATP and adenosine release during ischaemia in the mammalian hippocampus1. *J Neurochem* 2007; 101: 1400–1413.
30. ChamorroÁ, Dirnagl U, et al. Neuroprotection in acute stroke: targeting excitotoxicity, oxidative and nitrosative stress, and inflammation. *Lancet Neurol* 2016; 15: 869–881.
31. Pedata F, Dettori I, Coppi E, et al. Purinergic signalling in brain ischemia. *Neuropharmacology* 2016; 104: 105–130.
32. Di Virgilio F, Ceruti S, et al. Purinergic signalling in inflammation of the central nervous system. *Trends Neurosci* 2009; 32: 79–87.
33. Skaper SD, Debetto P and Giusti P. The P2X7 purinergic receptor: from physiology to neurological disorders. *FASEB J* 2010; 24: 337–345.
34. North RA. The molecular physiology of P2X receptors. *Physiol Rev* 2002; 82: 1013–1067.
35. Yan Z, Khadra A, Li S, et al. Experimental characterization and mathematical modeling of P2X7 receptor channel gating. *J Neurosci* 2010; 30: 14213–14224.
36. Locovei S, Bao L and Dahl G. Pannexin 1 in erythrocytes: function without a gap. *PNAS* 2006; 103: 7655–7659.
37. Iglesias R, Dahl G, Qiu F, et al. Pannexin 1: the molecular substrate of astrocyte "hemichannels". *J Neurosci* 2009; 29: 7092–7097.
38. Randhawa PK and Jaggi AS. Gadolinium and ruthenium red attenuate remote hind limb preconditioning-induced cardioprotection: possible role of TRP and especially TRPV channels. *Naunyn Schmiedebergs Arch Pharmacol* 2016; 389: 887–896.
39. Hamilton NB, Kolodziejczyk K, et al. Proton-gated Ca(2+)-permeable TRP channels damage myelin in conditions mimicking ischaemia. *Nature* 2016; 529: 523–728.
40. Jain S and Sharma B. Effect of ruthenium red, a ryanodine receptor antagonist in experimental diabetes induced vascular endothelial dysfunction and associated dementia in rats. *Physiol Behav* 2016; 164: 140–150.
41. Lindquist BE and Shuttleworth CW. Spreading depolarization-induced adenosine accumulation reflects metabolic status in vitro and in vivo. *J Cereb Blood Flow Metab* 2014; 34: 1779–1790.
42. Liu W, Ao Q, Guo Q, et al. miR-9 Mediates CALHM1-activated ATP-P2X7R signal in painful diabetic neuropathy rats. *Mol Neurobiol* 2016, 54: 922–929.